Roles of RIPK1/RIPK3 homo- and hetero-dimerization in cell death and pro-inflammatory signaling

A thesis submitted by

Xuzhong Yang

In partial fulfillment of the requirements for the degree of

Master of Science

in

Pharmacology and Drug Development

Tufts University

May 2017

Adviser: Alexei Degterev Ph.D.

Abstract

Necroptosis, a form of regulated necrosis, has been reported to be involved in numerous inflammatory diseases including multiple sclerosis, ischemia reperfusion injury, atherosclerosis, inflammatory bowel syndrome, and pancreatitis. Two homologous Ser/Thr kinases, receptor-interacting protein 1 (RIPK1) and RIPK3, play an important role in mediating necroptosis. RIPK1 and RIPk3 form heterodimeric amyloid scaffold through their RIP homotypic interaction motif (RHIM) domains, which serves as the platform for the downstream mixed lineage kinase domain-like (MLKL) mediated cell death and Erk1/2 mediated pro-inflammatory signaling induced by LPS. It is reported that RIPK3 homo-dimerization is sufficient to induce cell death in L929 and MEF cell lines. But it is still unclear how RIPK1/RIPK3 homo- or hetero-dimerization work on the pro-inflammatory signaling. In this study, we use FKBP-FRB-AP21976 inducible dimer system to artificially control the formations of different dimers between RIPK1 (RHIM domain mutated to avoid interaction with endogenous RIPK1/3) and RIPK3 (RHIM domain mutated) in L929 and RAW264.7 cells. We confirmed that RIPK3 homo-dimerization, rather than RIPK1 homo- or RIPK1/RIPK3 hetero-dimerization, could cause 40% cell death in L929 cell line. In the first several test sets, RIPK1 homo-dimerization could induce the expression of a number of pro-inflammatory mRNAs, including CSF2, CCL5, CXCL2 and this induction would be abolished by adding Nec-1s, the inhibitor of RIPK1 or SCH772984, the inhibitor of Erk1/2. However, this response was eventually lost, likely due to FKBP-RIPK1/FRB-RIPK1 aggregation

without dimerizer AP21976. In the RAW264.7 cells, there is no cell death or inflammatory signaling induction after dimerization, which may indicate the requirement for RHIM in these cells. The establishment of cell lines expressing inducible FKBP-FRB RIPK1 (wild type RHIM) is ongoing.

Table of Contents

List of Figures

List of Tables

List of Abbreviations

Caspase	cysteine dependent aspartate-directed protease
DMEM	Dulbecco's modified eagle medium
DMSO	dimethyl sulfoxide
Erk1/2	extracellular signal-regulated kinase 1/2
FADD	Fas-associated protein with death domain
FBS	fetal bovine serum
FKBP	FK506 binding protein
FRB	FKBP-rapamycin binding domain
IP	immunoprecipitation
MLKL	mixed lineage kinase domain-like protein
Nec-1	necrostatin-1
PBS	phosphate-buffered saline
RHIM	RIP homotypic interaction motif
RIP1	receptor-interacting protein 1
RIP3	receptor-interacting protein 3
ROS	reactive oxygen species
SDS	sodium dodecyl sulphate
SOC	Super Optimal broth with Catabolite repression
TBST	Tris-buffered saline with Tween-20
TNF	tumour necrosis factor
TNFR1	tumour necrosis factor receptor type 1
TRADD	TNFR1-associated death domain protein

Chapter 1: Introduction

Cell death can be divided into apoptosis and necrosis according to morphological changes. Apoptosis is a well-studied programmed mechanism of cell death, which follows a well-designed pathway that focuses on a cysteine-dependent aspartate-directed protease (caspase) cascade, accompanied by blebbing, cell shrinkage, nuclear fragmentation, chromatin condensation, chromosomal DNA fragmentation[1]. Apoptosis is activated either through an intrinsic or extrinsic pathway. In the intrinsic pathway, the cell kills itself because it senses cell stress, involving the cytochrome c release from mitochondria and the Apaf-1 complex formation that activates caspase-9, which in turn activates executioner caspase-3. In the extrinsic pathway, the cell kills itself because of signals from other cells: After the stimulation of death receptors (such as The FAS receptor and TNFR1), these receptors recruit caspase-8, which then processes the executioners of apoptosis, including caspase-3 and 7[2].

Necrosis is characterized by cell rounding, cell volume increase, organelle swelling, and the bursting of the cytoplasmic membrane, which has long been considered as a passive, un-programmed cell death resulting from cellular damage, overwhelming stress to cells or infiltration by pathogens. However, the discovery that the receptor-interacting protein kinase 1 and 3 (RIPK1 and RIPK3)-regulated cell death, termed necroptosis, possess necrotic phenotype totally changes this misconception[3-5]. Necroptosis is caspase-independent, but RIPK1 and RIPK3-dependent and is mediated by mixed lineage kinase domain-like (MLKL) protein[3]. Necroptosis can be triggered

by stimulation of several receptors including the tumor necrosis factor receptor (TNFR), Toll-like receptors (TLR3 and TLR4), or the T cell receptor (TCR) in the absence of active caspase-8[6-9]. Necroptosis is well studied in the context of the pleiotropic cytokine TNF (Figure 1.1)[10-13].

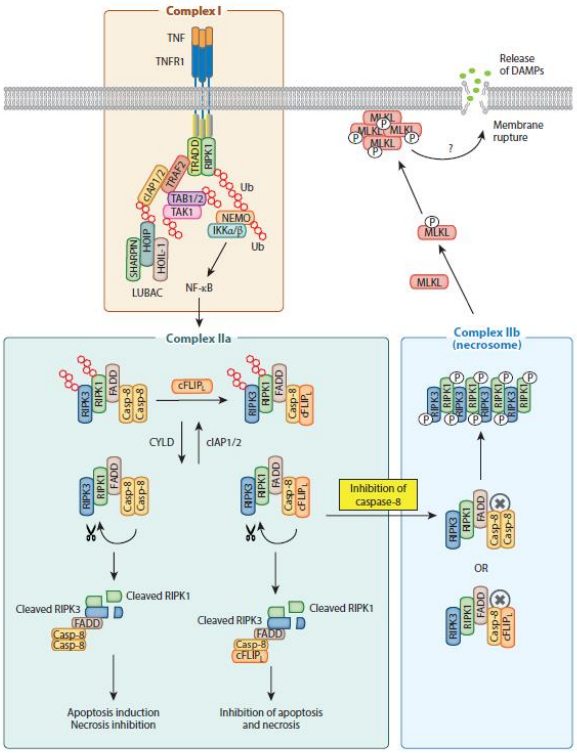

Figure 1.1 The schematics of TNF-induced signaling complexes

The interaction of TNF and TNF receptor 1 (TNFR1) results in the formation of the multi-protein complex: TNFR1 recruits TNFR-associated death domain (TRADD), NFR-associated factor 2 (TRAF2) and RIPK1 through its death domain[14, 15]. TRAF2 binds to a cellular inhibitor of apoptosis proteins 1 and 2 (cIAP1/2), recruiting the linear ubiquitin chain assembly complex (LUBAC). LUBAC serving as a scaffold recruits the TAB-transforming growth factor-activated kinase 1 (TAK1) complex and

IκB kinase (IKK) subunit NEMO to form TNFR1 complex 1[16-18]. After TNF complex activation, acting as an E3 ubiquitin ligase, cIAPs polyubiquitinate RIPK1 at lysine 63[16]. Therefore, the cell death functions of RIPK1 is blocked until it is recognized by deubiquitinating enzyme cylindromatosis (CYLD).[19, 20] Deubiquitinated RIPK1 released from the TNFR1 complex I could bind to the Fas-associated protein with a death domain (FADD), and then form TNFR1 complex II with caspase-8[21]. Activated caspase-8 is able to cleave RIPK1, by which it inhibits necroptosis and promotes apoptosis.[22] However, when caspase-8 is blocked (such as the pan-caspase inhibitor, Z-VAD), RIPK1 recruits RIPK3 via RIP homotypic interaction motif (RHIM) domain and then the two kinases auto-phosphorylate. RIPK1 and RIPK3 form an amyloid complex, which could be the core of the necrosome complex. The RHIM domain, existing in both RIPKI and RIPK3, is a critical domain for the formation of amyloid complexes. The RIPK1/RIPK3 amyloid complex is a major platform for recruiting other components and downstream effectors, such as mixed lineage kinase domain-like pseudokinase (MLKL). Then activated RIPK3 phosphorylates the pseudokinase MLKL, and activated MLKL could cause cell death[23].

Phosphorylated MLKL oligomerizes and translocates to the cell membrane. There is a four-helical bundle domain at the N-terminal of MLKL, which could recognize the lipid rafts rich in phosphatidylinositol phosphates on the cell membrane.[24-26] Active MLKL forms a pore in the cell membrane, which disrupts the ionic homeostasis of the cells and eventually causes cell death[27]. However, the exact ions (sodium; calcium;

magnesium) that relate to this process are controversial[28].

The serine/threonine kinases RIPK1 and RIPK3 are critical in cell death decisions and pro-inflammatory signaling. Our group recently showed that RIPK1 and RIPK3 mediate LPS-induced (TLR-4) pro-inflammatory gene expression, including IL1-α and TNFα in vitro and in vivo[29]. In contrast to RIPK1 and RIK3 regulated cell death, the inflammatory signaling is MLKL independent, and Erk1/2, TBK1/IKKε are involved in this signaling. The RIPK1/RIPK3 amyloid complex serves as the platform that controls both pro-death (mediated by MLKL) and pro-inflammatory (mediated by Erk1/2, TBK1, IKKε) downstream signaling[29].

The RIP1-RIP3 heterodimeric amyloid complex is believed to function as a platform that brings downstream signaling proteins into proximity to allow their activation[30]. This RIPK1/RIPK3 structural scaffold is critical for the downstream signaling. Disruption of this amyloid scaffold would result in the lack of auto-phosphorylation and activation of RIPK1 and RIPK3 and abolish the necroptosis pathway[13]. However, RIP1 and RIP3 also can each form dimer fibrils by their own RHIM domains in vitro[30]. By using FRB-FKBP inducible dimerization systems, Wu et al[30] recently showed homodimerization of RIP3 is sufficient to trigger its autophosphorylation and then recruit MLKL to execute necroptosis.

Numerous proteins and kinases perform their activities in the form of a dimer. A lot of dimerization systems were designed to artificially control the association and dissociation of protein dimers.

In my project, I focus on one of these dimerization methods, the FRB-FKBP/rapamycin

heterodimer formation system. Rapamycin is an antifungal antibiotic macrolide. It can bind to the 12-kDa FK506 binding protein (FKBP) and the FKBP-rapamycin binding (FRB) domain of the mammalian target of rapamycin (mTOR) at the same time, inducing the formation of FKBP-FRB hetero-dimer (Kd is around 2.5nM)[31].

The roles of homo- and hetero-RIPK1/RIPK3 interactions in the regulations of pro-inflammatory signaling is still unclear. We hypothesize RIPK3-RIPK3 homo-dimerization is sufficient to trigger cell death, but RIPK1 plays an important role in mediating inflammatory signaling. Hence, our objectives are to first get the different cell lines with different dimerization systems (FKBP-RIPK1/FRB-RIPK1; FKBP-RIPK1/FRB-RIPK3; FKBP-RIPK3/FRB-RIPK3) by Lentivirus infection, and second, by using AP21967 (rapamycin analog)-induced dimerization system, examine if RIPK1/RIPK3 homo-dimers or RIPK1-RIPK3 hetero-dimers are responsible for cell death or pro-inflammatory signaling.

Chapter 2: Methods and Materials

2.1 Cells

Lenti-X 293T, L929, and RAW264.7 cells were maintained in DMEM supplemented with 10% fetal bovine serum (FBS; Sigma, St. Louis, MO, USA) and 1% antibiotic-antimycotic mixture (Invitrogen, Carlsbad, CA, USA) at 37℃ and 5% CO2 in a humidified environment.

2.2 Cell death assay

Cell death was analyzed using CellTiter-Glo Luminescent Cell Viability Assay kit (Promega, Madison, WI, USA). The Luminescent Cell Viability Assays were performed according to the manufacturer's instruction. In brief[30], cells (150000/mL) were seeded in 96-well plate with white walls (Nunc). Cells were treated the next day. After treatment, an equal volume (15 μL/well) of Cell Titer Glo reagent was added to the cell culture medium, which had been equilibrated to room temperature for 30 min, cells were then incubated at room temperature for 20 min. Luminescent recording was then performed. The % of cell loss was determined by % of ATP loss. The ATP amount of AP21967-treated sample was normalized to that of the mock-treated sample, which was regarded as 100%. Results are presented as the mean ± S.E.M.

2.3 Protein Extraction and Western Blots

For Western blot experiments[29], 2,000,000 cells were seeded into 35 mm^2 dishes and then cultured overnight. Cells were washed with ice-cold PBS and lysed using lysis buffer including protease inhibitors (20 mM Tris-HCl, pH7.5, 150 mM NaCl, 1 mM Na_2EDTA, 1 mM EGTA, 1% Triton X-100, 2.5 mM sodium pyrophosphate, 1 mM β-glycerophosphate, 1 mM Na3VO4, 5 μg/ml Phenylmethanesulfonyl fluoride (PMSF) (Sigma), 1μg/ml leupeptine, 1μg/ml pepstatin and 1μg/ml aproprotinin). The cell lysates were centrifuged at 1000 g for 15 min, and then protein quantification in supernatants was done with Pierce 660 nM Protein Assay reagent (Thermo Scientific), and protein concentrations were adjusted to the same level. 60 μL of normalized protein

supernatant was added to 20 μl of 4×SDS loading sample buffer, with β-mercaptoethanol, to make WB sample with a total volume of 80 μL. For co-immunoprecipitation, supernatants were incubated overnight with 20 μL anti-Flag antibody beads at 4 ℃. Bead-protein-antibody mixtures were washed 3 times using lysis buffer. Bound proteins were eluted using SDS, samples were then heating up at 100 ℃ for 5 min. Beads were retrieved using the magnetic stand and solubilized protein was analyzed by Western blotting. Samples were separated by SDS/PAGE and transferred to PVDF membranes (activated by methanol in advance). Membranes were blocked in Protein-free T20 (TBS) blocking buffer (Fisher Scientific) at room temperature for 1 h, and incubated at 4 ℃ overnight with primary antibodies (1:1000 dilution in blocking reagent). The following day, membranes were washed with TBST buffer 3 times and incubated with secondary antibody (1:5000 dilution) at room temperature for 1 h. After washing by TBST 3 times, signals were developed using Luminata Classico or Forte HRP substrates (Millipore). To develop the film, the membrane was exposed to film in the dark room at various times, depending on the antibody.

2.4 DNA constructs

Lentiviral vectors encoding HA-FRB-RIPK1/RIPK3 (mutated RHIM domain) and Flag-FKBP- RIPK1/RIPK3 (mutated RHIM domain) were obtained from Dr. Han Jiahuai. HA-FRB-RIPK1/RIPK3 (mutated RHIM domain) and Flag-FKBP-RIPK1/RIPK3 (mutated RHIM domain) DNA fragments were inserted into lentiviral pLVX-IRES-zsGreen/mCherry vectors. Plasmids were isolated by Zyppy™ Plasmid

Mini prep Kit or QIAGEN Plasmid Midi prep kit.

Miniprep was conducted according to the protocol: 1. 5 mL of bacterial culture grown in LB medium were centrifuged for 5 min to get the bacterial pellet, and then discard the supernatant was discarded and re-suspended in 600 µL by RNase-free water. 2. 100 µl of 7X Lysis Buffer (Blue) was then added the and the sample was mixed by inverting the tube several times. After addition of 7X Lysis Buffer, the solution changed from opaque to clear blue, indicating complete lysis. 3. 350 µl of cold Neutralization Buffer (Yellow) was added into the tube. The sample was inverted for an additional 2-3 times to ensure complete neutralization. 4. The sample was centrifuged at 11,000 - 16,000 g for 2-4 minutes. 5. The supernatant (~900 µl) was transferred into the provided Zymo-Spin™ IIN column avoiding disturbing the cell debris pellet. 6. The column was placed into a Collection Tube and centrifuged for 15 seconds. 7. The flow-through was discarded and the column was placed back into the same Collection Tube. 8. 200 µl of Endo-Wash Buffer was added into the column and then centrifuged for 30 seconds. 9. 400 µl of Zyppy™ Wash Buffer was added to the column. Centrifuge for 1 minute. 10. The column was transferred into a clean 1.5 ml microcentrifuge tube then 30 µl of RNase free water was added directly to the column matrix and let stand for one minute at room temperature. 11. The plasmid DNA was eluted by 30 seconds centrifugation.

To mutate the RHIM domain back to wild type, the PfuUltra II Fusion HS DNA Polymerase (Agilent) was used:

dH2O	40.5 µL
10 Pfu Ultra reaction buffer	5.0 µL

dNTP mix (25 mM each)	0.5 μL
DNA template (100 ng/μL)	1.0 μL
Primer 1 (10 μM)	1.0 μL
Primer 2 (10 μM)	1.0 μL
Pfu Ultra DNA polymerase	1.0 μL
Total volume	50 μL

Table 2.1 Reaction Mixture for Mutagenesis PCR Amplification

Number of Cycles	Temperature ℃	Duration
1	92	2 min
30	92	30 seconds
	Primer Tm -5	30 seconds
	68	30 seconds per kb
1	68	10 minutes

Table 2.2 PCR Cycling Parameters for PfuUltra II fusion HS DNA Polymerase

Dpn I digestion: 0.2μL Dpn I enzyme (10 U/μL) was then added into the PCR reaction mix tube. Dpn I enzyme specifically recognizes methylation sites, which is used to remove the normally double-stranded template DNA. Mix it completely, incubate in 37 ℃ for 2 hours.

The transformation was performed following the NEB Stable Competent E. coli protocol with a few changes: 1. a tube of NEB Stable Competent E. coli cells was thawed on ice 2. 2 μL Dpn I treated product was added into the cell mixture. The tube

was flicked 4-5 times to mix cells and DNA. 3. Then the mixture was placed on ice for 30 minutes. 4. After 30 minutes ice incubation, the mixture was heat-shocked at exactly 42 ℃ for 30 seconds. 5. The mixture was placed back on ice for 5 minutes. 6. The tube was placed at 30 ℃ and shaking horizontally at 250 rpm for 60 minutes after adding 950 µl of room temperature SOC medium. 7. An ampicillin selection plate was warmed to 30 ℃. 8. After 3 minutes 1000g centrifugation, the pellet was re-suspended by 100 µL LB media. Then 100 µl of cells was spread onto a selection plate. Sequencing: The monoclonal colonies were picked and the plasmids were extracted for sequencing after 24 hours incubation at 37 ℃.

2.5 Lentivirus Production

Viral packaging (psPAX2) vector and viral envelope (pMD2G) vector were used. Lipofectamine 3000 Transfection Reagent (Invitrogen) was used to transfect plasmids into Lenti-X 293T cells. The experiment was conducted according to the protocol with some changes:

1. Lenti-X 293T cells were seeded onto 6-well or 10 cm culture plates at 70-80% confluence (for 6-well plates: 1,200,000 cells per well in 2mL of DMEM medium; for 10 cm plates: 3,000,000 cells per plate in 10 mL medium).

2. Cells were incubated overnight at 37 ℃, 5% CO_2.

3. At the second day, cell density was about 95-99% confluent. Opti-MEM I Reduced Serum Medium was pre-warmed to room temperature and Tube A and Tube B were prepared as described in the following tables:

Tube A	6-well plate	10cm plate
Opti-MEM I Reduced Serum Medium	250µL	500µL
Lipofectamine 3000 Transfection Reagent	7µL	14µL
Tube B	6-well plate	10cm plate
Opti-MEM I Reduced Serum Medium	250µL	500µL
P3000 Enhancer Reagent	6µL	12µL
psPAX2	5µg	10µg
pMD2G	1.77µg	3.54µg
pLenti expression vector	5µg	10µg

Table 2.3 Tube A and Tube B Mixture for Lipo 3000 transfection

4. The complexes were incubated for 10-20 minutes at room temperature.

5. Prior to adding complex, half of medium was removed from each well or plate, leaving a total of 1mL in each well or 5mL each 10 cm plate.

6. 500µL of lipid-DNA complex was added to each well or 1mL to each plate, taking care to dispense liquid against the well wall to avoid disrupting cells. Gently agitate plate to evenly distribute.

7. The plates were incubated for 6 hours at 37 ℃, 5% CO_2.

8. At 6 hours post-transfection, the medium was changed from each well or plate.

9. The plates were returned to the incubator, and incubated overnight at 37 ℃, 5% CO_2.

10. At 24 hours post-transfection, the cell supernatant was collected from each well or plate and stored in 15mL conical tubes at 4 ℃, which was the first batches of the virus.

11. The collected medium was replaced with pre-warmed DMEM medium. The plates were incubated overnight at 37 ℃, 5% CO_2.

12. Approximately 60 hours post-transfection, the second batches of the virus were collected.

13. The collected supernatant was centrifuged at 2,000 rpm for 10 minutes at room temperature to remove cellular debris. The supernatant was collected and the cell pellet was discarded.

14. The clarified supernatant was transferred into a sterile container and 1 volume of Lenti-X Concentrator was combined with 3 volumes of clarified supernatant. The tube was inverted several times.

15. The mixture was incubated at 4 ℃ overnight.

16. The mixture was centrifuged at 1500 g for 45 minutes at 4 ℃. After centrifugation, an off-white pellet was visible.

17. The supernatant was carefully removed without disturbing the pellet. The pellet was gently re-suspended in 100 μL PBS. The pellet was somewhat sticky at first but then went into suspension quickly.

2.6 Infection of cell lines

For L929 cells, 1. Cells were seeded onto 24-well plate at a density of 40,000 cells per well (30-50% confluent). 2. Before infection, the medium was changed into serum free. 20 uL virus and polybrene at a final concentration at 8 μg/mL were added into each well. 3. Then the plate was spun at 2,000 rpm at room temperature for 60 minutes. 4.

Another infection was repeated.

RAW264.7 cells were also seeded onto 24-well plate at a density of 40,000 cells per well. 6 uL ViroMag R/L reagent was added into 40 uL virus. ViroMag R/L is a magnetic nanoparticles formulation able to concentrate the virus particles onto cells within minutes. The mixture was incubated for 15 minutes at room temperature. Then, the ViroMag R/L/virus mixture was added into the cells. The cell culture plate was placed upon the magnetic plate for 15 minutes. The magnetic plate was removed and the cells were cultivated under standard conditions overnight. The infection was repeated for one more time.

2.7 RNA isolation, cDNA synthesis, and qRT-PCR

As Najjar et al described[29], cells were seeded onto 12-well plate at 150000/well. Total RNA was isolated using RNA MiniPrep kit (ZYMO Research) according to the manufacturer's protocol. RNA was then converted to cDNA by iScript cDNA Synthesis Kit (Bio Rad). qRT-PCR reactions were performed in LightCycler 480 II ((Roche, Nutley, NJ, USA) using VeriQuest SYBR Green master mix (Affymetrix) by the following conditions: 50 ℃ for 2 min, 95 ℃ for 10 min, followed by 40 cycles of 95 ℃ for 15 s and 60 ℃ for 1 min, followed by a hold at 4 ℃. Raw data can then be analyzed with LightCycle 480 Software version 1.5.0 SP3, generally using the automatic cycle threshold (Ct) setting for assigning baseline and threshold for Ct determination. The primer sequences used to amplify murine genes are as described in previous work[29]. All experiments were repeated with three independent biological replicas. For qRT-

PCR data, one representative data set is typically shown. Data shown represent the means ± SEM.

2.8 Flow Cytometry and Cell Sorting

Cells were washed three times with PBS, digested with trypsin at 37 ℃ for 5 min, collected by centrifugation at 1,400 rpm for 5 min, re-suspended into 1 ml of DMEM medium, and finally applied to flow cytometer for FACS analysis or sorting. The successfully infected cells expressing exogenous fusion proteins were sorted by flow cytometry based on GFP/mCherry expression.

Chapter 3: Results

3.1 Expression of fusion proteins

To artificially control different homo- or hetero dimerization of RIPK1/RIPK3,4 different L929 cell lines were established by lentivirus infection: cell line 1 only express endogenous RIPK1 and RIPK3; cell line 2 express FKBP-RIPK1, FRB-RIPK1 and endogenous RIPK1/RIPK3; cell line 3 express FRB-RIPK1, FKBP-RIPK3 and endogenous RIPK1/RIPK3; cell line 4 express FKBP-RIPK3, FRB-RIPK3 and endogenous RIPK1/RIPK3. The previous work showed that RHIM domain contributes to the polymerization of RIPK1 and RIPK3, and death domain in RIPK1 is critical for the dimer formation[30]. To avoid the interaction with endogenous RIP kinases, the RIHM domains in the fusion RIPK1 and RIPK3 were mutated (RIPK1 QIG529-531AAA; RIPK3 QIG449-451AAA) and the C-terminal death domains in the fusion RIPK1 were also deleted (Figure 3.1).

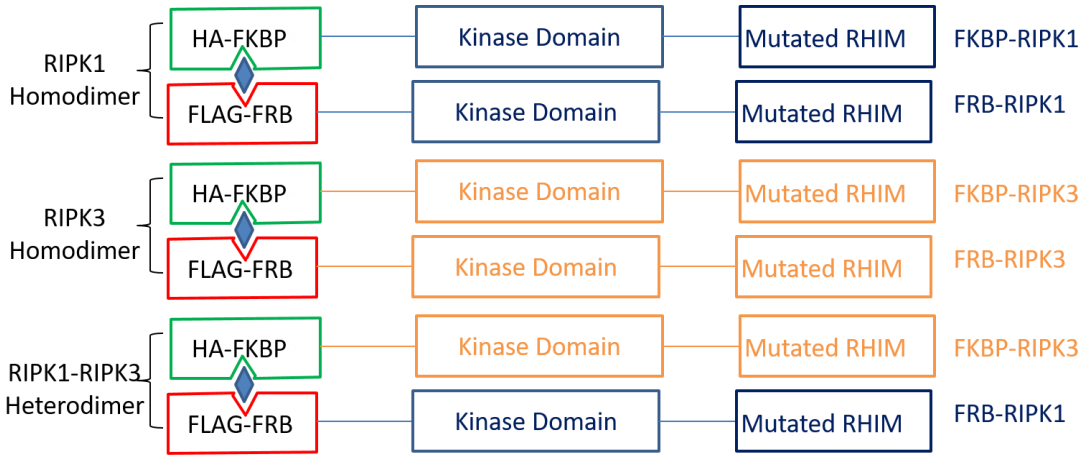

Figure 3.1 The schematics of RIPK1/RIPK3 fusion proteins and dimerization systems

Therefore, after AP21976 treatment, cell line 2 forms RIPK1 homo-dimer; cell line 3

forms RIPK1-RIPK3 hetero-dimer; cell line 4 forms RIPK3 homo-dimer and cell line 1 serves as the control.

Figure 3.2 confirmed the expression of different fusion proteins in 4 L929 cell lines by Western blot. The FRB-RIPK1 fusion protein (death domain deleted) has the similar size as endogenous RIPK1, making the two bands merge together in Western blot.

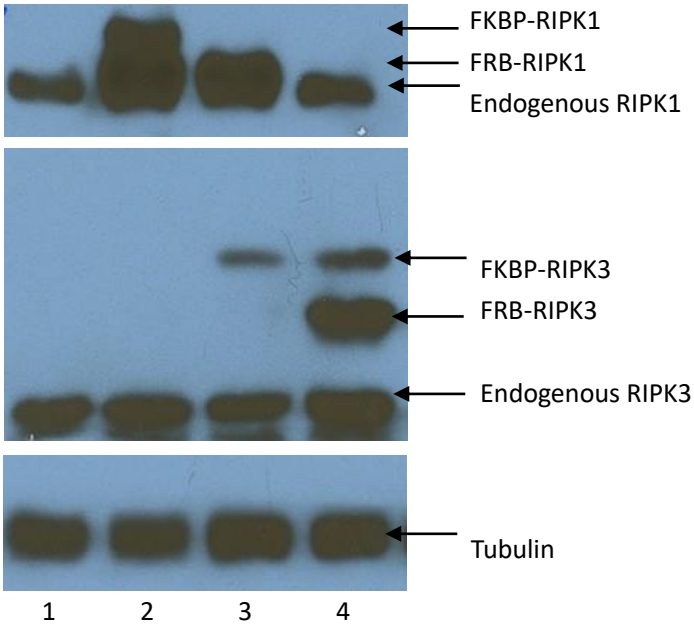

Figure 3.2 Western blot of the fusion protein expressions in different cell lines

3.2 Examining the FKBP/FRB/AP21976 dimerization system

Since all the four L929 cell lines expressed the fusion proteins as we designed, the very next step was to verify whether the FKBP/FRB dimerization system works or not. We use cell line 4 to test it. Figure 3.3 showed that the fusion protein Flag-FRB-RIPK3 in the cell line 4 was pulled down by anti-Flag antibody. After AP21976 treatment, HA-FKBP-RIPK3 was also pulled down together with Flag-FRB-RIPK3, suggesting the interaction between FKBP- and FRB- fusion proteins in the presence of AP21976.

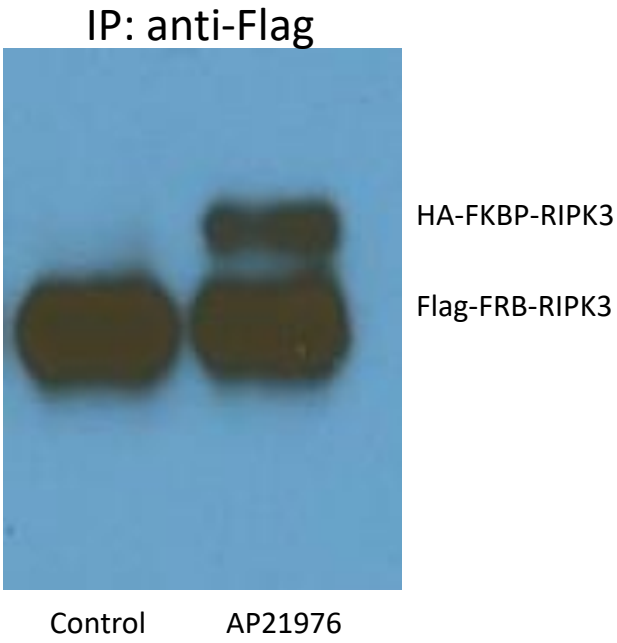

Figure 3.3 Western blot of the Flag IP for cell line 4

3.3 RIPK3 homo-dimerization triggers L929 cell death

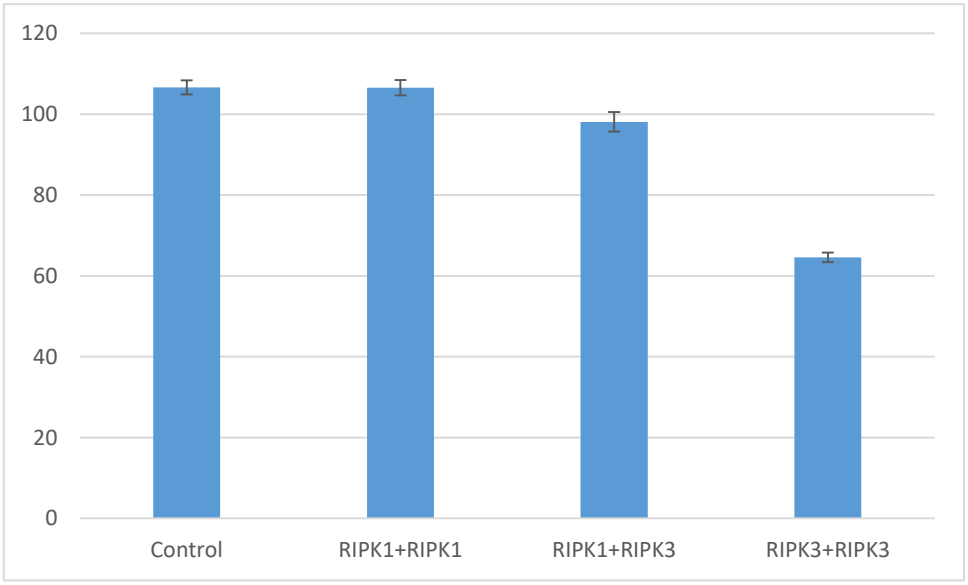

Figure 3.4 The L929 cell viability after 250 nM AP21976 treatment

After treating the L929 cells with 250 nM AP21976 for 16 hours, the cell viabilities were detected by CellTiter-Glo reagent. Figure 3.4 indicated that neither RIPK1 homo-

dimerization nor RIPK1/RIPK3 hetero-dimerization could induce cell death, however, around 40% cell died when RIPK3 homo-dimerized, which was consistent with the previous result[30].

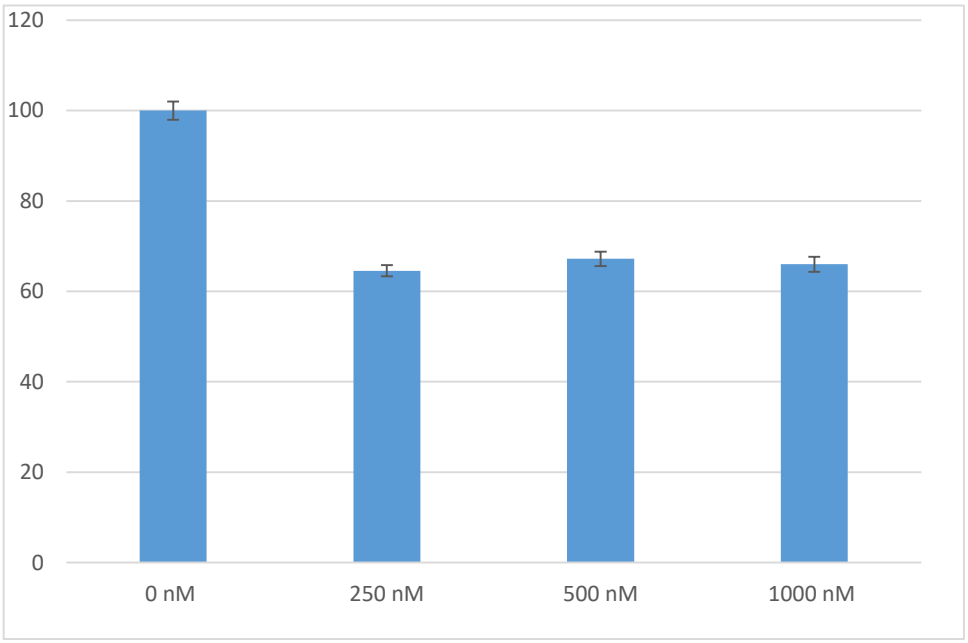

Figure 3.5 The cell viability under different concentrations of AP21976 treatments

Furthermore, we evaluated the effect of different concentrations of AP21976 on cell death. Figure 3.5 showed that even the concentration of AP21976 varies from 250 nM to 1000 nM, the percentage of cell death didn't change, which was about 40% (16 hours). This result indicated that 250 nM AP21976 is sufficient to trigger the dimerization of FKBP and FRB in this case, and the cell death is not AP21976 concentration-dependent when the concentration is higher than 250 nM.

3.4 The effect on pro-inflammatory signaling expression after dimerization

The results of this part varied greatly. The results from different test sets showed different conclusions, but these data also lead to some interesting thinking.

The expression of inflammatory mRNAs in L929 cells was assessed by qRT-PCR. The results of first several tests demonstrated that the RIPK1 homo-dimerization induced the expression of a number of inflammatory mRNAs.

After 250 nM AP21976 treatment for 8 hours, the CSF2 (GM-CSF) mRNA level in different L929 cell lines were measured. Figure 3.6 showed that only RIPK1-RIPK1 homo-dimerization could induce the expression of CSF2. The CSF2 mRNA expression level increased about 7.9~10.1 fold compared to the control at 8 hours' time point. At 24 hours after adding 250 nM AP21967, the CSF2 mRNA level increased about 30 fold (Figure 3.7).

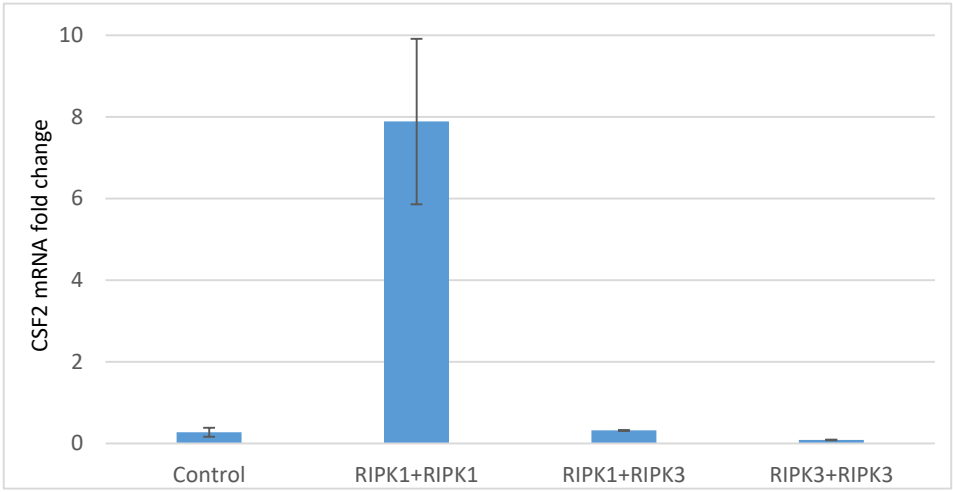

Figure 3.6 The expression of CSF2 in 4 different L929 cell lines after AP21976 treatment

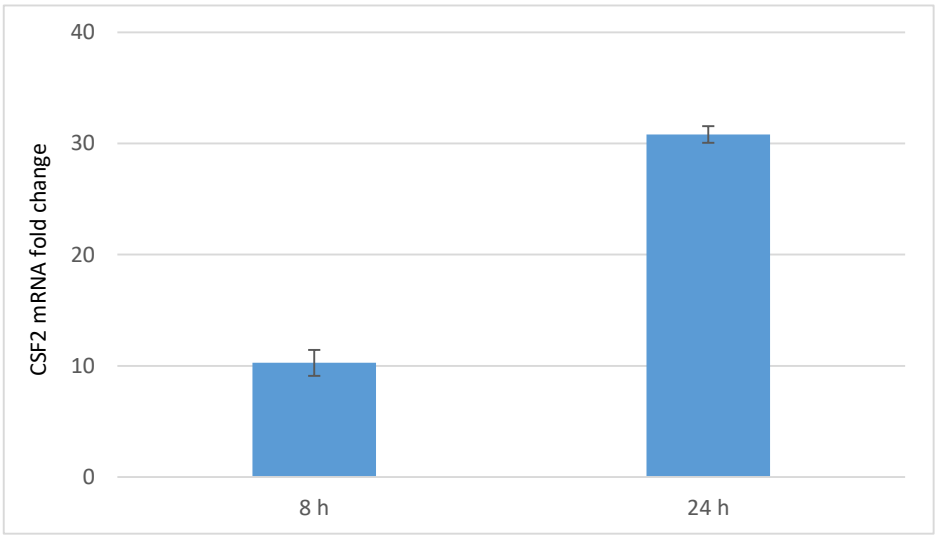

Figure 3.7 The expression of CSF2 at different time points after AP21976 treatment

Then, a panel of other inflammatory mRNAs level in L929 cell line 2 (RIPK1+RIKP1) was also tested after 250 nM AP21976 treatment for 8 hours. Figure 3.8 showed that several mRNAs expression in L929 cells were upregulated after RIPK1 homo-dimerization, including CCL5 (RANTES), CXCL5, and especially CXCL2.

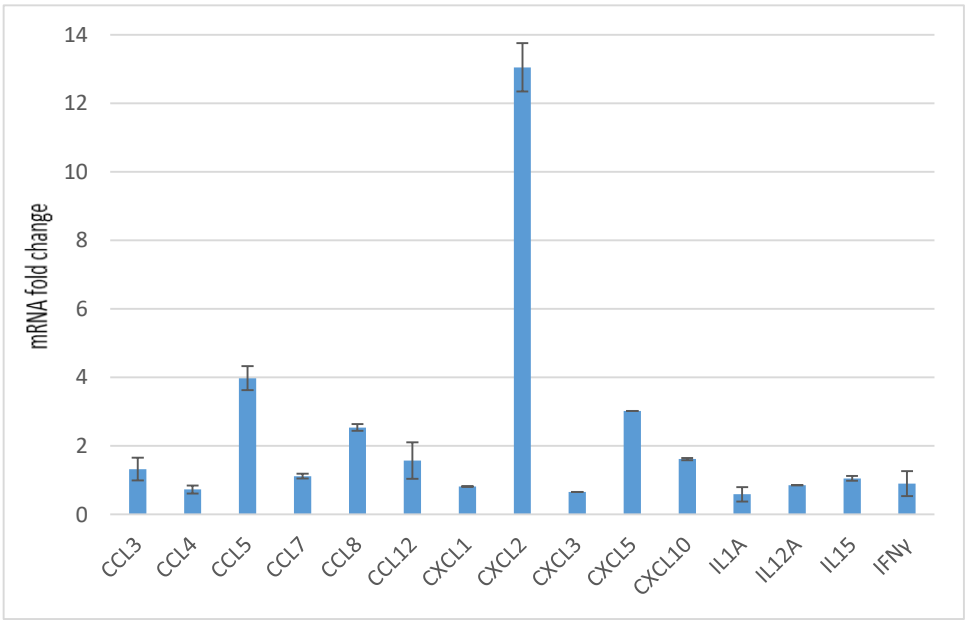

Figure 3.8 The expression of CSF2 in 4 different cell lines after AP21976 treatment

Among all the inflammatory mRNAs tested, CSF2 and CXCL2 showed relatively high

induction after RIPK1 homo-dimerization, therefore, the mRNA levels of CSF2 and CXCL2 were detected in the inhibitor test.

L929 cells were treated by AP21976 in the presence of 3 inhibitors relatively: RIPK1 inhibitor Nec-1s; RIPK3 inhibitor GSK'872; Erk1/2 inhibitor SCH772984. The upregulations of CSF2 and CXCL2 after AP21976 treatment were abolished by RIPK1 and Erk1/2 inhibitors (Figure 3.9), suggesting that the kinase activity of RIPK1 and Erk1/2 are indispensable in the pro-inflammatory signaling induced by RIPK1 homo-dimerization.

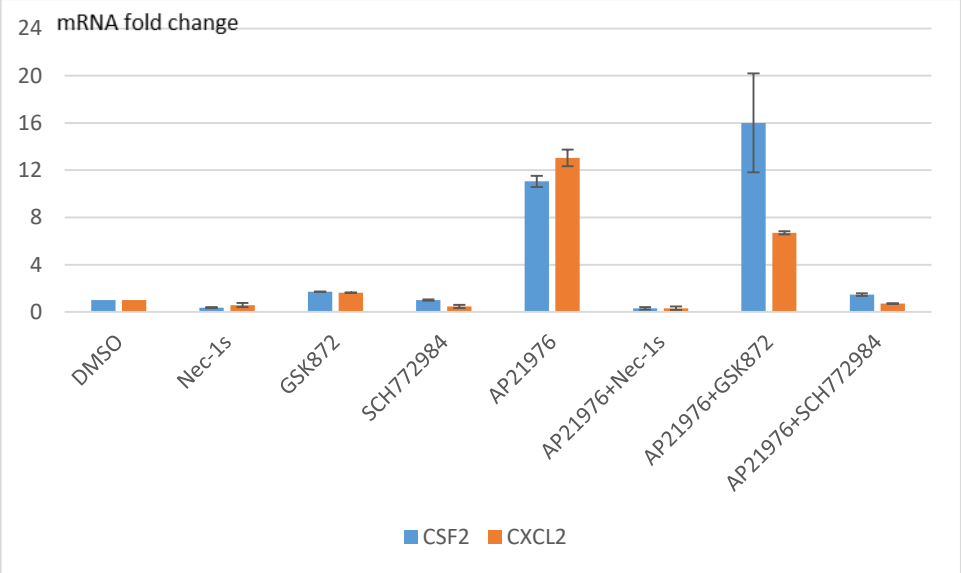

Figure 3.9 The expression of CSF2 and CXCL2 in the presence of different inhibitors

However, in the later tests, the mRNA expressions of CXCL2 and CSF2 in the cell line 2 (RIPK1+RIPK1) after AP21976 treatment did not show much upregulations (Figure 3.10) compared to without AP21976. Looking at the qRT-PCR data carefully, we found out that the CSF2 and CXCL2 mRNA levels in cell line 2 (RIPK1+RIPK1) were much higher than that in cell line 1 (empty control) even without AP21976 treatment. Figure

3.11 showed that, without AP21976, the CSF2 level in cell line 2 was 18 fold higher than that in cell line 1, and the CXCL2 level was 11 fold higher.

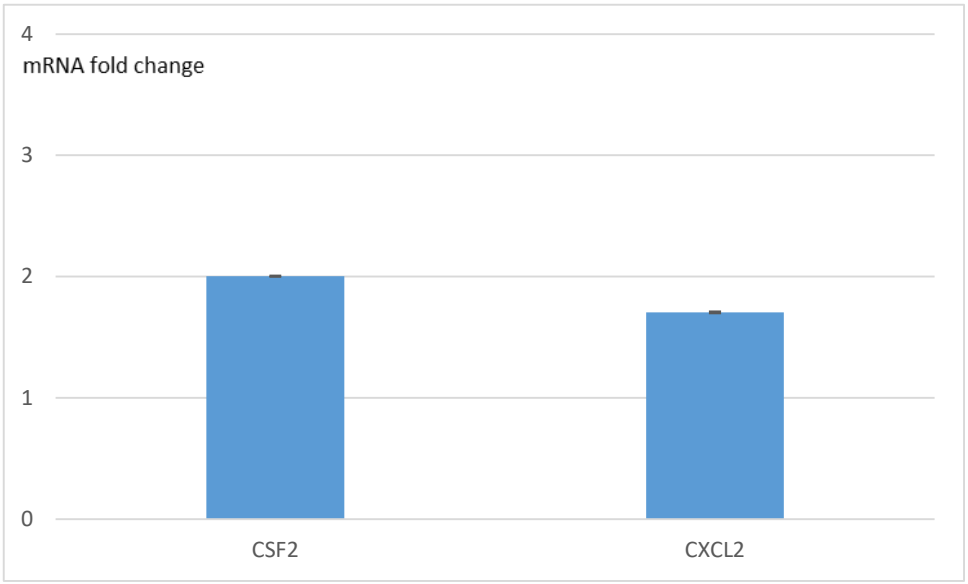

Figure 3.10 The expression of CSF2 and CXCL2 in the later experiments

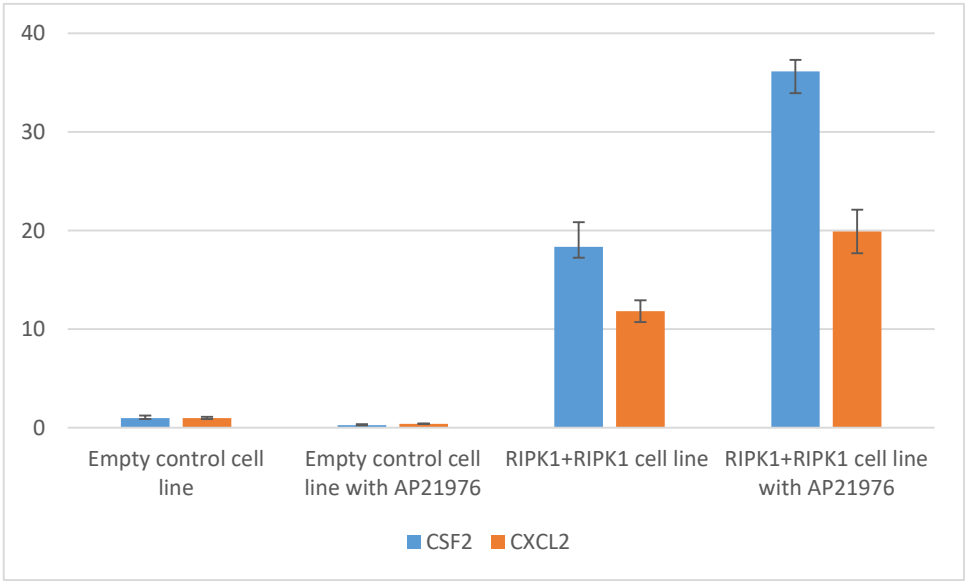

Figure 3.11 The expression of CSF2 and CXCL2 in cell line 1 and 2 with or without AP21976

To figure out this problem, the Western blot experiment was carried out. Figure 3.12 showed that Flag-FRB-RIPK1 fusion protein was pulled down by anti-Flag antibody

beads, however, the HA-FKBP-RIPK1 fusion protein was pulled down as well, suggesting FRB-RIPK1 and FKBP-RIPK1 formed aggregates even without AP21976.

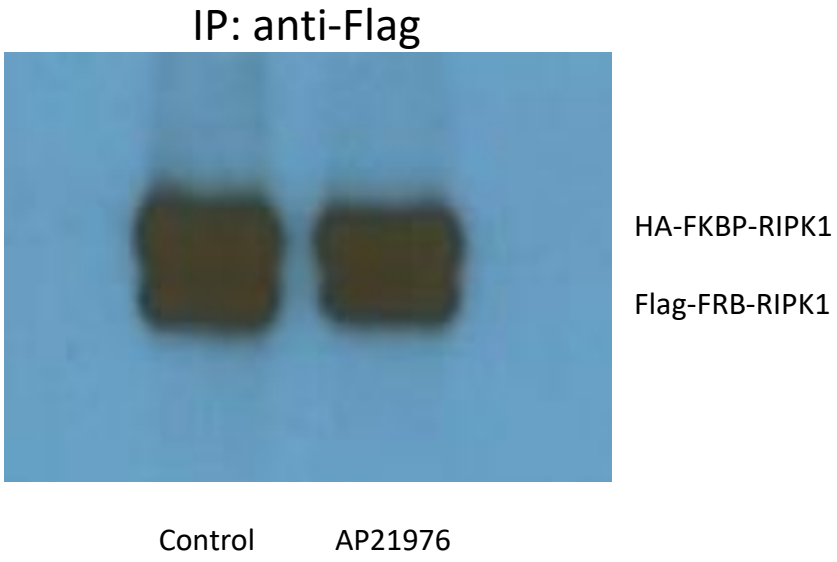

Figure 3.12 Western blot of the Flag IP for cell line 2

Based on the above data, I speculated that when the cell line 2 was just obtained, the FKBP-RIPK1 and FRB-RIPK1 fusion proteins could not form the dimer due to the lack of death domain and the mutated RHIM domain. When adding AP21976, RIPK1 formed dimer because of the interaction of FKBP and FRB, followed by the downstream inflammatory signaling. Four L929 cell lines were kept in regular DMEM medium with 1:10 splitting every 3 days. However, after several passages, the FKBP-RIPK1 and FRB-RIPK1 in cell line 2 gradually autonomously formed aggregates (unknown cause) and induced the expression of inflammatory mRNAs, so that after the addition of AP21976, CSF2 and CXCL2 expression didn't increase significantly.

Four RAW264.7 cell lines were also constructed. Cell line 1: empty control; cell line 2: FKBP-RIPK1 + FRB-RIPK1; cell line 3: FRB-RIPK1 + FKBP-RIPK3; cell line 4:

FKBP-RIPK3 + FRB-RIPK3. Like the four L929 cell lines, in four RAW264.7 cell lines, all the RIHM domain in the fusion RIPK1 and RIPK3 were mutated (RIPK1 QIG529-531AAA; RIPK3 QIG449-451AAA) and the C-terminal death domains in the fusion RIPK1 were deleted. However, after AP21976 treatment, none of the four cell lines detected cell death and no significant increase in the expression of inflammatory mRNAs (Figure 3.13, 3.14).

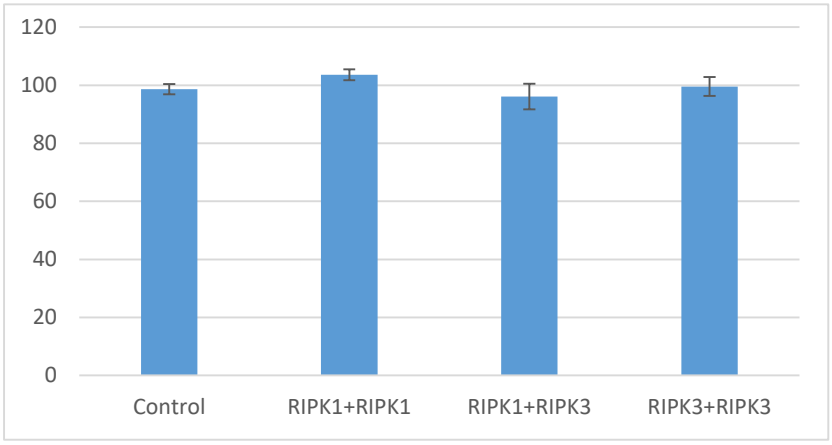

Figure 3.13 The RAW264.7 cell viability after 250 nM AP21976 treatment

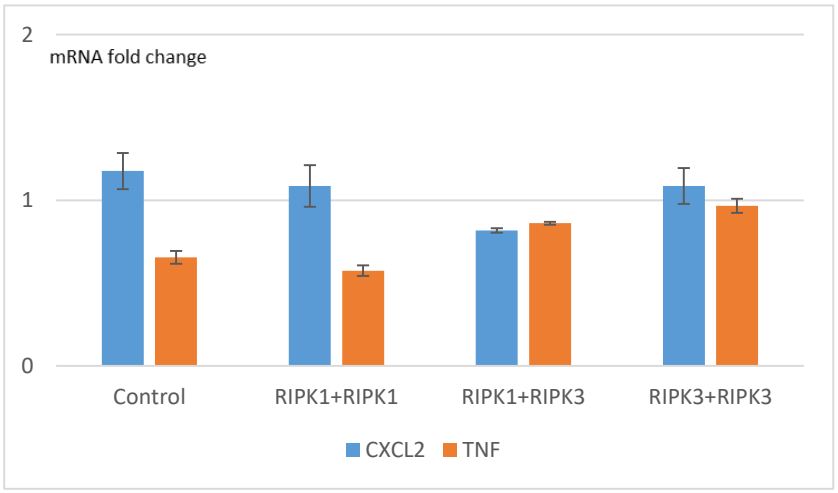

Figure 3.14 The expression of CXCL2 and TNFα in 4 different RAW264.7 cell lines after AP21976 treatment

3.5 To establish the new cell lines (WT RHIM domain)

In RAW264.7 cells, we hypothesized that the activity of RHIM domain is essential in RIPK1/RIPK3-mediated cell death and pro-inflammatory signaling. We then reconstructed RAW264.7 cell line expressing GFP-FKBP-RIPK1+mCherry-FRB-RIPK1 (WT RHIM domain). At the same time, we also constructed new L929 cell line expressing GFP-FKBP-RIPK1+mCherry-FRB-RIPK1 (WT RHIM domain).

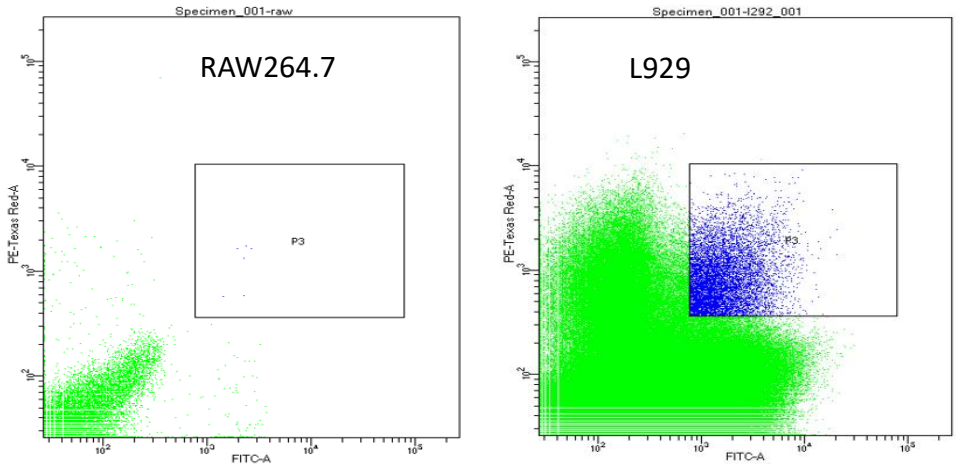

Figure 3.15 The first sorting of RAW264.7 and L929 cells

After infection, fluorescent cells were isolated by Fluorescent Activated Cell Sorting (FACS). In Figure 3.15, the X-axis represents the green fluorescent intensity, and the Y-axis stands for the red fluorescent intensity. The cells located in gate P3 suggested the co-expression of GFP and mCherry fusion proteins, which were likely GFP-FKBP-RIPK1 and mCherry-FRB-RIPK1. Figure 3.15 showed that about 1% L929 cells were double positive, and less than 0.1% RAW264.7 cells were double positive. 40 days after first sorting, fluorescent cells were analyzed by FACS (Figure 3.16). The cells in R7 area were double positive with both GFP and mCherry fusion proteins expression. Only

29.56% RAW264.7 cells and 42.39% L929 were double positive, suggesting many cells are not stable at expressing inserted genes. Therefore, the second sorting was conducted (Figure 3.16). The cell population locating in R3 gate with the strong green and red fluorescence was isolated.

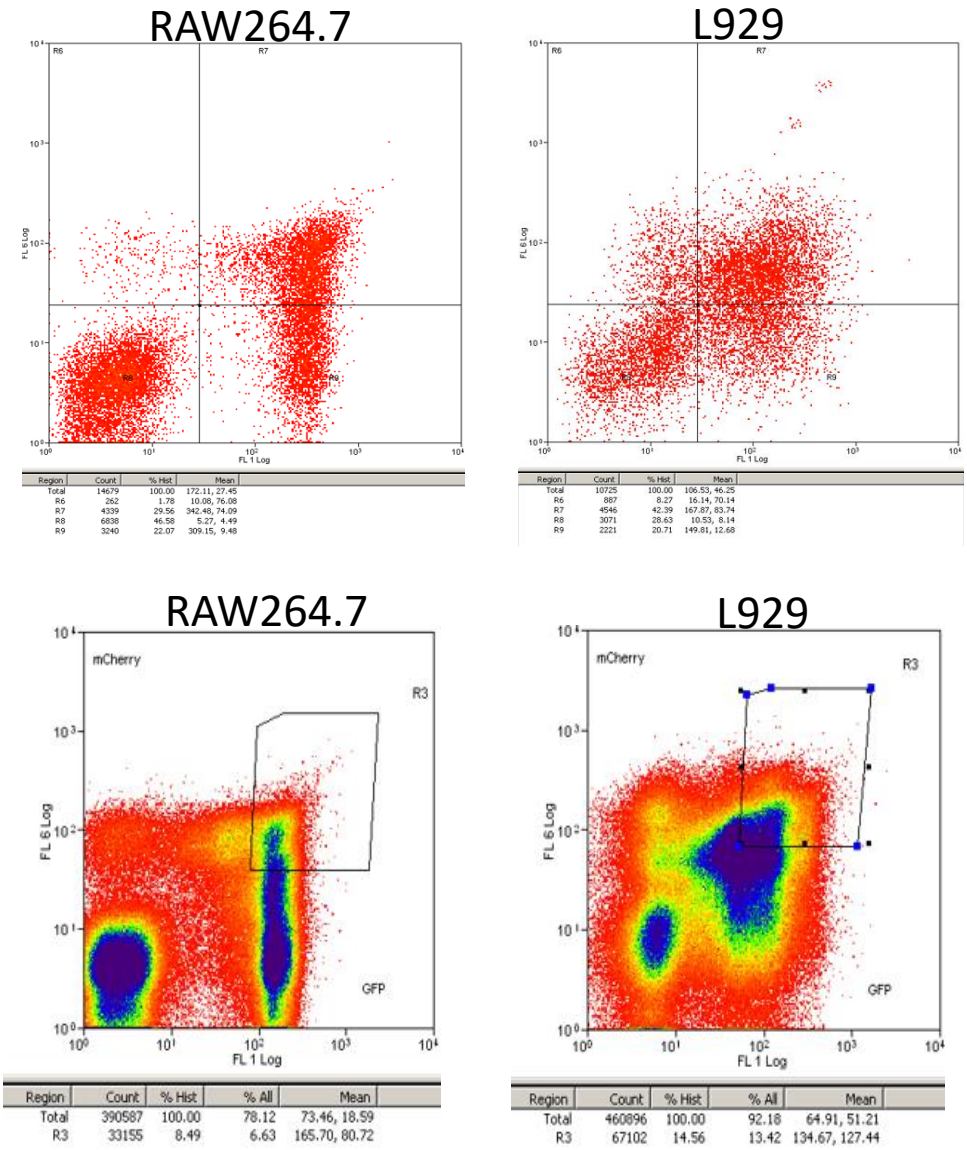

Figure 3.16 The second sorting of RAW264.7 and L929 cells

Chapter 4: Discussion

In this study, FKBP-FRB-AP21976 inducible dimer systems were established in L929 and RAW264.7 cell lines by lentivirus infection. Infection efficiency is very low, especially in RAW264.7 cells. Prior to the first sorting, the double positive rate of FKBP/FRB-RIPK1 RAW264.7 cell was less than 0.1%. There may be two reasons for the low efficiency of infection: 1. RAW264.7 is a macrophage cell line, which is difficult to transduce with lentivirus; 2. the inserted genes, especially RIPK1, are not very compatible with RAW264.7 cells since the double positive rate of the control group can reach 10%. In addition, after the first sorting, the second sorting need to be carried out because many cells are not stable at expressing inserted genes.

There are some limitations in this study. For L929 cells, FRB-RIPK1/FKBP-RIPK3; FKBP/FRB-RIPK3 and FKBP/FRB-RIPK1 dimer systems should be tested working or not immediately after obtaining four L929 cell lines by Flag-IP Western Blot. However, I only tested FKBP/FRB-RIPK3. Due to the lack of Western blot data, we were unable to draw a solid conclusion that RIPK1 homo-dimerization induces pro-inflammatory signaling from the initial qRT-PCR results. I speculate that FKBP-RIPK1 and FRB-RIPK1 did not form aggregates without AP21976 when the cell line 2 was just established, and the addition of AP21976 dimerized RIPK1, triggering downstream inflammatory signaling induction. However, after several passages, FKBP-RIPK1 and FRB-RIPK1 formed aggregates even without AP21976. If the speculation is true, the CXCL2 and CSF2 mRNA levels in cell line 2 without AP21976 would be significantly

decreased in the presence of Nec-1s, RIPK1 inhibitor or SCH772984, Erk1 / 2 inhibitor. After sorting, L929 cells were cultured under regular condition with 1 to 10 splitting every 3 days. The induction of pro-inflammatory mRNAs expression in cell line 2 (RIPK1 homo-dimer) gradually decreased, and eventually disappeared, however, the cell death rate induced by AP21976 in cell line 4 (RIPK3 homo-dimer) was keeping at 40%, suggesting the RIPK3 dimerization system was still inducible.

For RAW264.7 cells, we didn't confirm the dimerization systems after obtaining the cell lines by FACS sorting, therefore the conclusions for RAW264.7 cells are preliminary. We did not detect the cell death or inflammatory signaling induction after dimerization, suggesting that the activity of RHIM might be indispensable in RAW264.7 cells or the dimerization systems are not compatible with RAW264.7 cells with a view to the extremely low double positive ratio. Therefore, establishing the RAW264.7 cell line expressing FKBP/FRB-RIPK1 (wild type RHIM domain) is very important.

For the future direction, the establishment of RAW264.7 cell line expressing FKBP/FRB-RIPK1 (wild type RHIM domain) is ongoing. Besides, it would be very interesting to figure out why FKBP/FRB-RIPK1 dimerization system didn't work after several passages while the FKBP/FRB-RIPK3 dimerization system was still inducible.

Chapter 5: Bibliography

1. Fink, S.L. and B.T. Cookson, *Apoptosis, pyroptosis, and necrosis: mechanistic description of dead and dying eukaryotic cells.* Infect Immun, 2005. **73**(4): p. 1907-16.
2. Hengartner, M.O., *The biochemistry of apoptosis.* Nature, 2000. **407**(6805): p. 770-776.
3. Christofferson, D.E. and J. Yuan, *Necroptosis as an alternative form of programmed cell death.* Curr Opin Cell Biol, 2010. **22**(2): p. 263-8.
4. Degterev, A., et al., *Chemical inhibitor of nonapoptotic cell death with therapeutic potential for ischemic brain injury.* Nat Chem Biol, 2005. **1**(2): p. 112-9.
5. Silke, J., J.A. Rickard, and M. Gerlic, *The diverse role of RIP kinases in necroptosis and inflammation.* Nat Immunol, 2015. **16**(7): p. 689-97.
6. He, S., et al., *Toll-like receptors activate programmed necrosis in macrophages through a receptor-interacting kinase-3-mediated pathway.* Proc Natl Acad Sci U S A, 2011. **108**(50): p. 20054-9.
7. Tenev, T., et al., *The Ripoptosome, a signaling platform that assembles in response to genotoxic stress and loss of IAPs.* Mol Cell, 2011. **43**(3): p. 432-48.
8. Upton, J.W., W.J. Kaiser, and E.S. Mocarski, *DAI/ZBP1/DLM-1 complexes with RIP3 to mediate virus-induced programmed necrosis that is targeted by murine cytomegalovirus vIRA.* Cell Host Microbe, 2012. **11**(3): p. 290-7.
9. Kaiser, W.J., et al., *Toll-like receptor 3-mediated necrosis via TRIF, RIP3, and MLKL.* J Biol Chem, 2013. **288**(43): p. 31268-79.
10. Cho, Y.S., et al., *Phosphorylation-driven assembly of the RIP1-RIP3 complex regulates programmed necrosis and virus-induced inflammation.* Cell, 2009. **137**(6): p. 1112-23.
11. He, S., et al., *Receptor interacting protein kinase-3 determines cellular necrotic response to TNF-alpha.* Cell, 2009. **137**(6): p. 1100-11.
12. Zhang, D.W., et al., *RIP3, an energy metabolism regulator that switches TNF-induced cell death from apoptosis to necrosis.* Science, 2009. **325**(5938): p. 332-6.
13. Chan, F.K., N.F. Luz, and K. Moriwaki, *Programmed necrosis in the cross talk of cell death and inflammation.* Annu Rev Immunol, 2015. **33**: p. 79-106.
14. Harper, N., et al., *Fas-associated death domain protein and caspase-8 are not recruited to the tumor necrosis factor receptor 1 signaling complex during tumor necrosis factor-induced apoptosis.* J Biol Chem, 2003. **278**(28): p. 25534-41.
15. Micheau, O. and J. Tschopp, *Induction of TNF receptor I-mediated apoptosis via two sequential signaling complexes.* Cell, 2003. **114**(2): p. 181-90.
16. Bertrand, M.J., et al., *cIAP1 and cIAP2 facilitate cancer cell survival by functioning as E3 ligases that promote RIP1 ubiquitination.* Mol Cell, 2008. **30**(6): p. 689-700.
17. Ea, C.K., et al., *Activation of IKK by TNFalpha requires site-specific ubiquitination of RIP1 and polyubiquitin binding by NEMO.* Mol Cell, 2006. **22**(2): p. 245-57.
18. Haas, T.L., et al., *Recruitment of the linear ubiquitin chain assembly complex stabilizes the TNF-R1 signaling complex and is required for TNF-mediated gene induction.* Mol Cell, 2009. **36**(5): p. 831-44.
19. Wu, P., et al., *The LEF1/CYLD axis and cIAPs regulate RIP1 deubiquitination and trigger apoptosis in selenite-treated colorectal cancer cells.* Cell Death Dis, 2014. **5**: p. e1085.

20. Feoktistova, M., et al., *cIAPs block Ripoptosome formation, a RIP1/caspase-8 containing intracellular cell death complex differentially regulated by cFLIP isoforms.* Mol Cell, 2011. **43**(3): p. 449-63.
21. Wang, L., F. Du, and X. Wang, *TNF-alpha induces two distinct caspase-8 activation pathways.* Cell, 2008. **133**(4): p. 693-703.
22. Lin, Y., et al., *Cleavage of the death domain kinase RIP by caspase-8 prompts TNF-induced apoptosis.* Genes Dev, 1999. **13**(19): p. 2514-26.
23. Li, J., et al., *The RIP1/RIP3 necrosome forms a functional amyloid signaling complex required for programmed necrosis.* Cell, 2012. **150**(2): p. 339-50.
24. Cai, Z., et al., *Plasma membrane translocation of trimerized MLKL protein is required for TNF-induced necroptosis.* Nat Cell Biol, 2014. **16**(1): p. 55-65.
25. Dondelinger, Y., et al., *MLKL compromises plasma membrane integrity by binding to phosphatidylinositol phosphates.* Cell Rep, 2014. **7**(4): p. 971-81.
26. Murphy, J.M., et al., *The pseudokinase MLKL mediates necroptosis via a molecular switch mechanism.* Immunity, 2013. **39**(3): p. 443-53.
27. Su, L., et al., *A plug release mechanism for membrane permeation by MLKL.* Structure, 2014. **22**(10): p. 1489-500.
28. Xia, B., et al., *MLKL forms cation channels.* Cell Res, 2016. **26**(5): p. 517-28.
29. Najjar, M., et al., *RIPK1 and RIPK3 Kinases Promote Cell-Death-Independent Inflammation by Toll-like Receptor 4.* Immunity, 2016. **45**(1): p. 46-59.
30. Wu, X.N., et al., *Distinct roles of RIP1-RIP3 hetero- and RIP3-RIP3 homo-interaction in mediating necroptosis.* Cell Death Differ, 2014. **21**(11): p. 1709-20.
31. Inobe, T. and N. Nukina, *Rapamycin-induced oligomer formation system of FRB-FKBP fusion proteins.* J Biosci Bioeng, 2016. **122**(1): p. 40-6.